Why our rainfall-runoff models keep underestimating the peak flows?

András Bárdossy[1] and Faizan Anwar[1]

[1]Institute for Water and Environmental System Modeling, University of Stuttgart, 70569 Stuttgart, Germany

Correspondence: Faizan Anwar (faizan.anwar@iws.uni-stuttgart.de)

Abstract.

In this paper the question of how interpolation of precipitation in space by using various spatial gauge densities affects the rainfall-runoff model discharge if all other input variables are kept constant is investigated. The main focus was on the peak flows. This was done by using a physically-based model as the reference with a reconstructed spatially variable precipitation and a conceptual model calibrated to match the reference model's output as closely as possible. Both models were run with distributed and lumped inputs. Results showed that all considered interpolation methods resulted in underestimation of the total precipitation volume and that the underestimation was directly proportional to the amount. More importantly, the under-estimation of peaks was very severe for low observation densities and disappeared only for very high density precipitation observation networks. This result was confirmed by using observed precipitation with different observation densities. Model runoffs showed worse performance for their highest discharges. Using lumped inputs for the models showed deteriorating performance for peak flows as well, even when using simulated precipitation.

1 Introduction

Hydrology is to a very large extent driven by precipitation, which is highly variable in space and time. Point precipitation is interpolated in space that is subsequently used as the true precipitation input for hydrological models without any further adjustments. A common problem with most interpolation schemes is that the variance of an interpolated field is always lower than the variance of the individual point data that were used to interpolate it. Another problem which is very important in the case of high precipitation events is that the absolute maximum precipitation coordinates in the interpolated field are at one of the observation locations. Contrary to reality, it is very unlikely that for any given precipitation event the maximum precipitation takes place at any of the observation locations. Accounting for conditional changes with additional variables helps only a little but never enough. New interpolations schemes are introduced on a regular basis but the main drawback is inherent to all of them. Furthermore, distribution of the interpolated values tends to Gaussian, with an increase in the number of observations used for interpolation for each grid cell, even when it is known that precipitation has an exponential-like distribution in space for a given time step and also for a point in time. From experience in previous studies, Bárdossy et al. (2022, 2020); Bárdossy and Das (2008), it was clear that model performance was dependent on the number and the configuration of observation station

locations but no decisive conclusion was made. It should not come as a surprise that models perform better, in terms of cause and effect, with increasing data quantity and quality.

The problem of less precipitation observations

The effects of taking a sample from a population on the final distribution of precipitation can be visualized in the following manner. Suppose, precipitation is measured at each point in space. For any given time step, when it is raining at some of the points, the distribution of values is exponential-like. Sampling a finite number of N values from the space, the chances that points are sampled from the upper tail become smaller and smaller as N approaches 1 or conversely samples from the lower tail are more likely. This has a strong bearing on the rainfall-runoff process. A large part of small rainfall volumes is intercepted by the soil and the vegetation. These do not influence the peak flows directly. Large flows in rivers are due to soil saturation during or after a rainfall event. To produce soil saturation and therefore runoff, a model first needs to be fed such large precipitation values. The saturation overflow is not necessarily catchment wide. It could also be due to a large precipitation event over part of the catchment. If the precipitation observation network is not dense enough, it is possible that a representative pattern of the event is not captured, even after interpolation due to the reasons mentioned before. Using this *false* precipitation as model input will consequently lead to producing less saturation overflow and thereby model runoffs not matching the the observed.

Objectives

To investigate the effects of sampling finite points in space on model performance and the reproduction of flood peaks this study tries to answer the following questions:

1. How strong is the effect of sampling density on the estimation of areal precipitation for intense precipitation events? Is there a systematic signal?

2. How does interpolation quality and hydrological model performance change with precipitation observation density?

3. How strong is the effect of an error in precipitation observations on discharge estimations?

4. What is the role of spatial variability of hydrological model performance? How much information is lost if areal mean precipitation is used i.e., sub-scale variability is ignored?

Some of the aforementioned points, among others, were recently discussed in a review paper by Moges et al. (2021). They highlighted four sources of hydrological model uncertainties: parameter, input, structural and calibration data uncertainty. Their conclusion was that out of the four, parameter uncertainty got the most attention. Even though, all of these sources contribute to the final results in their own unique manner.

Kavetski et al. (2003) concluded that addressing all types of uncertainty will force fundamental shifts in model calibration/verification philosophy. So far, the rainfall-runoff modeling community has not been able to put such ideas into common practice. The reason being that a true estimate of the uncertainty of a forever changing system is extremely difficult to find.

The so called epistemic uncertainty will always exist. Moreover, there is no consensus on how to model these uncertainties. Following Kavetski et al. (2003), Renard et al. (2010) showed that taking into account both input and structural uncertainty is an ill-posed problem as combinations of both affect the output and the performance of the model and addressing both simultaneously is not possible.

60　　Balin et al. (2010) tried to assess the impacts of having point rainfall uncertainty on model discharge by taking a 100 km^2 catchment at a spatial resolution of 200 m at a daily time scale. A normally distributed error of 10% was added to the observed time series to produce new time series. This was done multiple times independently. By running the model with the erroneous data (among other things), they found that the resulting performances were not so different than the original case. The only noticeable difference was that the uncertainty bounds on discharge were slightly wider resulting in more observed

65　values contained by it. The conclusion was that the causes of model output uncertainty may not be due to erroneous data as the measurement errors everywhere compensated for the runoff error in a way that the final model performance stayed the same. More interestingly, they found out that using observed rainfall for modeling resulted in under estimation of the peak flows, a problem that this study will also try to address. Furthermore, for the same catchment Lee et al. (2010) arrived at similar conclusions by using a different approach and a lumped rainfall-runoff model. Yatheendradas et al. (2008) investigated

70　uncertainty of flash floods using a physically-based distributed model by considering a mixture of parameter and input data uncertainty. They concluded that their model responses were heavily dependent on the properties of the precipitation estimates using radar, among other findings.

This study is a special case of model input uncertainty. It specifically deals with the effects of using interpolated precipitation data as a rainfall-runoff model input that is derived from point observations. It does not deal with input uncertainty as it is meant

75　to be as doing so requires very strong assumptions that are likely to remain unfulfilled, as was also pointed out in Beven (2021). The idea that various forms of uncertainties exist and should be considered is not disputed.

The rest of the study is organized as follows: Sect. 2 shows the investigation area and Sect. 3 shows the model setup, inputs and the main idea of this study in detail. Sect. 4 discusses the two rainfall-runoff models used in this study and the methods of their calibration. Sect. 5 discusses the results in detail where the questions posed in the beginning of this section are answered.

80　Sect. 6 presents two coarse correction approaches to reduce precipitation bias that were tried. Finally, in Sect. 7, the study ends with the summary, main findings and implications of the results.

2　Investigation area

The study area is the Neckar catchment situated in the South-West of Germany in the federal state of Baden-Würrtemberg (Fig. 1). It has a total area of 14,000 km^2. From the East it is bounded by the Swabian Alps and by the Black forest on the West.

85　The maximum elevation is ca. 1000 m in the Swabian Alps that goes down to 170 m at the confluence of the Neckar and Rhine in the North. Mean recorded temperature is about 9.1 °C while minimum and maximum ever recorded are -28.5 and 40.2 °C respectively. Annual precipitation sums reach to about 1800 mm in the Black Forest while the rest of the area receives 700

to 1000 mm on the mean. The probability of precipitation on a given day and at a specific location is ca. 50% with a mean precipitation of 2.5 mm per day.

The entire catchment area of the Neckar was not modeled by the considered rainfall-runoff models in this study. Rather, the large headwater catchments were modeled only, where times-of-concentration were long enough to allow for model runs on a daily resolution i.e., if a large precipitation events takes place then the ensuing peak in discharge is observed at the next time step. Namely, the Enz, Kocher and Jagst with catchment areas of 1656, 1943 and 1820 km^2 respectively. Other reasons for selection of these was that they are relatively intact as compared to the main river which is modified for transportation and also the fact the the effects of catchment boundaries (e.g., exact boundary line and exchanges with neighboring catchments) vanish as the size becomes larger.

3 Model input data preparation

Point meteorological data time series (daily precipitation, and temperature) were downloaded from the Deutscher Wetter Dienst's (DWD, German Weather Service) open access portal (DWD, 2019). The daily discharge time series was downloaded from the open access portal of the Landesanstalt für Umwelt Baden-Württemberg (LUBW, Environmental agency of the federal state of Baden-Württemberg) (LUBW, 2020). The considered time period is from 1991 to 2015. Furthermore, the precipitation gauges used in this study are evenly distributed across the catchment even at high elevations (Fig. 2). This is very important because one of the cited causes of precipitation volumes (e.g., Yang et al. (1999); Legates and Willmott (1990); Neff (1977)) is the smaller density of gauges at higher elevations. It is also important to note that effects of elevation on daily precipitation are negligible (Bárdossy and Pegram, 2013).

3.1 Precipitation interpolation using various gauge densities

To demonstrate the effects of various gauge densities on peak flows of models, time series of the existing precipitation network for the time period of 1991-2015 were taken. There were a total of 343 gauges. Only a subset of these was active at any given time step as old stations were decommissioned and new ones were commissioned. Out of the total, random samples of sizes 10, 25, 50, 100 and 150 gauge time series were selected and gridded precipitation was interpolated using these for each catchment that was subsequently lumped into a single value for each time step. This was done 100 times. For comparison, the same was done by using all the gauges. Furthermore, two interpolation schemes i.e., Nearest neighbor (NN) and Ordinary Kriging (OK) were used to show that the problem was not interpolation scheme dependant. A stable variogram fitting method that was described in Bárdossy et al. (2021) was used for OK.

3.2 Reference precipitation

In the previous case, precipitation interpolations were not compared to reality, as one cannot not know what the real precipitation was at locations with no stations. To obtain a complete coverage of rainfall, simulated precipitation fields were considered.

A realistic virtual dataset was created to investigate the effect of precipitation observation density instead of using interpolated precipitation. For this purpose, a 25 year long daily precipitation dataset corresponding to the time period of 1991-2015 was used. This dataset contains gridded precipitation on a 147x130 km grid with 1 km resolution. It was created so that the precipitation amounts were the same as the observed precipitation at the locations of the weather service observation stations. Additionally, the empirical distribution function of the entire field for any selected day is the same as that of the observations and its spatial variability (measured as the variogram) is the same as the observed. This precipitation is considered as *reality*. It is called *reference or reconstructed precipitation* throughout this text. Full details of the procedure are described in Bárdossy et al. (2022). To summarize the idea of the said study, consider the problem of inverse modeling in which a physically-based rainfall-runoff model is set up for a catchment. Daily fields of interpolated precipitation are fed to it, among other inputs. The model hydrograph is computed. It should come as no surprise that the model and observed runoff do not match. Assume that all the error in the model hydrograph are due to precipitation only. Now the question to be answered is that *what precipitation will result in a hydrograph that has very little to no error compared to the observed?* To do so, new realizations of precipitation that are constrained to have precipitation values exactly the same as those at the observation locations along with the same correlation function for any given time step in space are needed. The time step with a large error is selected and precipitation fields for the about 10 time steps before this are simulated and fed to the model as new inputs. The resulting error is checked. If it reduces, the new precipitation fields replace the old ones as observed. If not, then they are rejected and new ones are simulated and tested. This procedure is repeated up to the point where the model runoff error stops improving. Next, another time step is selected that is far away (more than 10 time steps) from the one rectified before and the same procedure is repeated for that one. In this way all the time steps are treated and a new time series of precipitation fields is obtained that has significantly less error compared to the case when interpolated precipitation is used.

3.3 Precipitation interpolation using the reference

To demonstrate the effects of sparse sampling of data and the resulting model runoff error, the following method was used: N number of points were sampled from the reference grid. Time series for each point (1x1 km cell) was then extracted and taken as if it were an observed time series. Care was taken to sample points such that the density was nearly uniform over the study area. N was varied to obtain a given amount of gauge density. Here, densities of 1 in 750, 400, 200 and 130 km^2 were used. These correspond to 25, 50, 100 and 150 cells out of the 19,110 respectively. Labels of the form MN, are used to refer to these in the figures, where M is a suffix to signify interpolation with N being the number of points used to create the interpolation. For reference, Germany has around 2000 active daily precipitation stations for an area of 360,000 km^2 which is about 1 station per 180 km^2. The random sampling was performed 10 times for each N in order to see the effects of different configurations later on in the analysis of the results.

This way many time series were sampled from the reference for various gauge densities. From here on the same procedure was applied that is normally used in practice i.e., Spatial interpolation. To keep things simple the Ordinary Kriging (OK) method was used to interpolate fields on the same spatial resolution as the reference at each time step. The use of OK is arbitrary. One could very well use any preferred method. Use of other methods that interpolate in space will not help much as

5

all of them tend to result in fields that have reduced variance as compared to the variance of the observed values. Moreover, it is also very unlikely (but possible in theory) that an interpolation scheme predicts an extreme at locations where no measurements were made.

3.4 Temperature and potential evapotranspiration

External Drift Kriging (EDK) (Ahmed and De Marsily, 1987) was used to interpolate daily observed minimum, mean and maximum temperature for all cells at a resolution similar to that of the precipitation with resampled elevation from the SRTM (Farr et al., 2007) dataset as the drift. For potential evapotranspiration (PET), the Hargreaves-Samani (Hargreaves and Samani, 1982) equation was used with the interpolated temperature data at each cell as input. It was assumed that temperature and potential evapotranspiration are much more continuous in space as compared to precipitation which behaves as a a semi-Markov process in space-time that has a much larger effect on the hydrograph in the short term. To clarify that the role of temperature and PET is not very important while considering peaks, consider the following: Peaks are a result of large scale precipitation. It could be due to continuous precipitation that is not very intense but persists longer in time or an intense event of a smaller duration. Long precipitation events result in very little sunlight and therefore little evapotranspiration. What is the effect of $2\ mm$ of evapotranspiration on a day where it rained $50\ mm$? An intense event will result in saturation of the soil and increased overland flow, again not enough time for evapotranspiration to have any significant impact. The only time when temperature may have a considerable effect is when it goes very low, a large snow event takes place for many days and then the temperature suddenly rises in the coming days rather quickly. It is very rare. For example, such an event that is on record in the study area took place in 1882. This was also investigated previously in Bárdossy et al. (2020). Even then, the effect of temperature is modelled to a very good extent by the interpolation due its nature in space-time.

4 Model setup

Two rainfall-runoff models, namely SHETRAN (Ewen et al., 2000) and HBV (Bergström, 1992), were considered in this study. Same gridded inputs were used for both and at a spatial resolution of 1x1 km and at a daily temporal resolution. Except for precipitation, all other inputs remained the same during all the experiments. Description of the model used and the setup specific to each is discussed in the following two subsections.

4.1 SHETRAN

SHETRAN is a physically based distributed hydrological model which simulates the major flows (including subsurface) and their interactions on a fine spatial grid (Ewen et al., 2000). It includes components for vegetation interception and transpiration, overland flow, variably saturated subsurface flow and channel–aquifer interactions. The corresponding partial differential equations are solved using a finite-difference approximation. The model parameters were not calibrated. Instead, available data such as the elevation, soil and land use maps were used to estimate the model parameters at a 1x1 km spatial resolution (Lewis et al., 2018; Birkinshaw et al., 2010). It was considered as a theoretically correct transformation of rainfall to runoff. This way,

combined with the reference precipitation, a realistic virtual reality was created in which the effect of different sampling densities could be investigated. Same SHETRAN settings were used for the various precipitation interpolations. Furthermore, the model and settings are the same as those in Bárdossy et al. (2022), which the readers are encouraged to read before proceeding further.

4.2 HBV

HBV is one of the most widely used models that needs no introduction. It requires very little input data i.e., precipitation, temperature and potential evapotranspiration. Each grid cell of HBV was assumed to be a completely independent unit. All cells shared the same parameters, only the inputs were different. The runoff produced by all cells was summed up at the end to produce the final simulated discharge value for each time step. It was calibrated for the reference precipitation and each of the precipitation interpolation. Differential Evolution (DE) (Storn and Price, 1997) was used to find the best parameter vector. It is one of the genetic-type optimization schemes to find the global optimum by updating a given sample of parameter vectors successively by mixing three in a specific manner. A population size of 400 was used to find the global optimum. Overall, it needed 150 to 200 iterations to converge for 11 parameters. 50% Nash-Sutcliffe (NS) (Nash and Sutcliffe, 1970) and 50% NS using the Natural logarithm (Ln-NS) was used as the objective function for calibration. Ln-NS was chosen because NS alone concentrates too much on the peak flows during calibration and disregards, almost 95% of, the remaining flows. Ln-NS helps to mitigate this flaw to some degree but not completely.

5 Results

Before showing the results, some terms specific to the following discussion are defined first. They are put here for the readers' ease.

1. The term *reference precipitation* refers to the reconstructed precipitation that is taken as if it were the observation. *Reference model* refers to SHETRAN with the reference precipitation as input and the resulting discharge of this setup is the *reference discharge*.

2. *Interpolated discharge* refers to the discharge of SHETRAN or HBV with interpolated precipitation as input. The model is mentioned specifically for it. The term *subsampling* refers to extraction of time series of a subset of points from the entire grid.

3. *Model performance*, refers to the value of the objective function whose maximum, and optimum, value is 1.0, anything less is *less* performance. The performance of the reference discharge is 1.

4. Furthermore, *discharge* and *runoff* are used interchangeably. They both refer to the volume of water produced by a catchment per unit time which is cubic meters per second in this study. The terms *observation station*, *gauge* and *station* are used interchangeably. These refer to the meteorological/discharge observation stations.

7

5.1 Metrics used for evaluation

To compare the change in precipitation or model runoff, scatter plots of reference values on the horizontal versus their corresponding values after interpolation on the vertical scale are shown. Each point represents lumped precipitation for all the cells i.e., mean of all the cells per time step.

The largest five aerially lumped values for precipitation in the reference and the values at the corresponding time steps in interpolation are compared by showing them as a percentage of the reference. This produces a number of points that is the product of the number of interpolations and the considered number of events. For comparing discharge, 5 largest values in the reference discharge are compared against the values at the same time steps using interpolated discharge. This results in 5 points per interpolation. Violin plots are used to show these points as densities.

Furthermore, figures comparing a high discharge event using all the interpolations are shown at the end of each subsection wherever relevant. Tables summarizing over- and under-estimations as percentages relative to the reference are shown at the end of each subsection.

5.2 Comparison of interpolations using fewer vs. all gauges

Comparison of the largest five precipitation events' depth using various number of gauges taken from the entire network are shown in Fig. 3 and 4 for Enz. These are normalized with respect to the values computed using the entire network (343 gauges). There are many cases where the fewer gauges' interpolations have larger values than the ones with the entire network. However, the more important point to notice is the bias. By using a lower number of gauges, underestimation of the largest precipitation events is more likely. NN exhibits a larger variance in terms of under- and over-estimations compared to OK. Using more gauges shows that the deviations reduce significantly. Another aspect that should be kept in mind is that here *interpolations* are compared to *an interpolation*. Even by using all the gauges, there is still a very high chance of missing the absolute maximum precipitation at a given time step. Keeping this in mind one should be aware that runoff predicted by a model using this *smoothed* precipitation with all the gauges will still produce, on average, smaller peaks. This will become clearer by the results in the next sections where the reference precipitation is used. Tables 1 and 2 summarize the cases with under- and over-estimations using various number of gauges with respect to using all of them for interpolation for the three catchments using NN and OK respectively.

5.3 Effects of subsampling from reference on precipitation

Fig. 5 shows an exemplary event with very high daily precipitation for the reference and various interpolation cases. For the lowest number of gauges, the field appears very smooth and has a smaller variance as compared to the field with the most stations which is much closer to the reference.

In Fig. 6, the scatter plot of lumped reference against one of the lumped interpolation values for all time steps for Kocher is shown. Here, it is interesting to notice that overall, the larger the value in reference, the more it is reduced by the interpolation. On the other hand, the interpolation increases the magnitude of the smaller values. Events in the mid-range values are

8

	10	25	50	100	150
Enz	60-09-31	51-16-33	45-26-29	35-41-24	25-52-23
Kocher	55-13-32	49-20-31	40-28-32	32-38-30	22-53-25
Jagst	52-15-33	48-20-32	40-28-32	32-36-32	25-53-22

Table 1. Relative percentages of under- and over-estimations of the top 5 precipitation events using various gauge densities (columns) with respect to the top 5 values using interpolation with all the gauges for the three considered catchments (rows) using NN. The values are of the format *percentage of underestimations (below 97.5%), within a threshold of ±2.5%, and overestimations (above 102.5%) with respect to the interpolation using all gauges*. For example, 60-09-31 in the first row and first column means that out of the 100 interpolations (with 5 events per interpolation) using 10 gauges for Enz, 60% of the events were below 97.5%, 9% were within 97.5% and 102.5%, and 31% were above 102.5% of the top 5 events using the interpolation with all the 343 gauges.

	10	25	50	100	150
Enz	66-09-25	56-18-26	50-29-21	36-43-21	24-56-20
Kocher	61-15-24	62-17-21	52-25-23	35-42-23	20-57-22
Jagst	60-12-28	57-20-23	50-29-21	39-40-22	24-60-15

Table 2. Under- and over-estimation percentages of the top 5 precipitation events using OK. Caption of Table 1 shows how to interpret the numbers here.

underestimated by a significant margin. Most points are below the ideal line. Consider the subsequent mass balance problems that would arise by such a consistent bias. Over the long term, one would adjust the model to have lower evapotranspiration. Over the short term, the peak flows would almost always be underestimated. It is important to keep in mind that high discharge values are the result of a threshold process in the catchment where the water moves in larger volumes towards the stream once the soil saturates or when the infiltration cannot keep up with the rainfall/melt intensity. To match the peaks in such scenarios, it is important to obtain the correct estimates of precipitation.

Fig. 7 shows the relative change of the largest five peak precipitation values. These were computed by dividing the interpolated precipitation by the reference at the time steps of the top 5 events. A consistent bias, i.e., underestimation, is clear. Especially, for the coarsest interpolation (25 points). Such a bias appears small but cosider the extra volume over a 1000 km^2 catchment that is not intercepted by the soil. Another interesting point to note is that for the other interpolations there are some overestimations as well. All the relative under- and over-estimations for the three catchments with various densities are summarized in Table 3.

	M025	M050	M100	M150
Enz	74-20-06	60-20-20	45-38-18	44-47-09
Kocher	80-06-14	60-18-22	50-15-35	31-44-24
Jagst	84-04-12	42-24-34	35-35-30	22-53-24

Table 3. Percentages of under- and over-estimations of the top 5 precipitation events using various gauge densities (columns) with respect to the top 5 values using reference precipitation for the three considered catchments (rows). The values are of the format *percentage of underestimations (below 97.5%), within a threshold of $\pm2.5\%$, and overestimations (above 102.5%) with respect to the reference precipitation.* For example, 31-44-24 in the second row and last column means that out of the 10 interpolations (with 5 events per interpolation) using 150 points for Kocher, 31% of the events were below 97.5%, 44% were within 97.5% and 102.5%, and 24% were above 102.5% of the top 5 events using the reference precipitation.

5.4 Effects of subsampling from reference on discharge of SHETRAN

Similar to the precipitation, systematic bias in model runoff was investigated next. Fig. 8 shows the resulting runoff by using the same precipitation (Fig. 6) as input to SHETRAN. What is immediately clear is that there are almost no overestimations of discharge values when using interpolated precipitation. The largest peak is reduced by almost 50%.

Looking at Fig. 9, the mean of the largest five peaks is reduced significantly while using the least number of points for Kocher. The other point to note is that the peaks drop on average for other interpolations (except for the last one) much more as compared to the reduction in precipitation. To see the effects more in detail, Fig. 10 and 11 show hydrographs obtained using various gauging densities for two events. It is very clear that as the gauging density rises, the underestimation decreases proportionally and the hydrographs become similar. All the under- and over-estimations are summarized in the Table 4 for all the catchments.

	M025	M050	M100	M150
Enz	80-02-18	78-06-16	60-28-12	49-27-24
Kocher	91-04-04	84-10-06	56-24-20	27-49-24
Jagst	76-04-20	62-18-20	56-28-16	38-38-24

Table 4. Percentages of under- and over-estimations of the top 5 discharge events using various gauge densities (columns) with respect to the top 5 values using reference discharge for the three considered catchments (rows) using SHETRAN. The values are of the format *percentage of underestimations (below 97.5%), within a threshold of $\pm2.5\%$, and overestimations (above 102.5%) with respect to the reference discharge.* For example, 38-38-24 in the third row and last column means that out of the 10 interpolations (with 5 events per interpolation) using 150 points for Jagst, 38% of the events were below 38%, 38% were within 97.5% and 102.5%, and 24% were above 102.5% of the top 5 events using the reference discharge.

5.5 Effects of subsampling from reference on discharge of HBV

While observing the scatter of reference and interpolated precipitation discharge in Fig. 12, HBV shows a different behaviour as compared to SHETRAN. Overestimations from low to high flows exist except for the largest high flows which are underestimated as well. Again, not as much as that by SHETRAN. This is due to the recalibration, where the new parameters compensate for the missing precipitation by decreasing evapotranspiration. This aspect will be investigated thoroughly in future research.

Fig. 13 shows the scaling of the five highest peaks compared to the reference discharge. Here, a similar reduction for the least amount of stations can be seen. Even for the highest number of stations, the discharges are still underestimated. This signifies that even a distributed HBV with full freedom to readjust its parameters cannot fully mimic the dynamics of the flow produced by SHETRAN. Hydrographs for the same events shown in the previous section for HBV are shown in Fig. 14 and 15. It is interesting to note that the first event is overestimated by all interpolations and that the hydrographs become similar as the gauging density increases. The second event is estimated better as the gauging density increases. All the under- and over-estimations are summarized in the Table 5 for all the catchments.

	M025	M050	M100	M150
Enz	78-04-18	78-04-18	78-02-20	71-00-29
Kocher	100-00-00	96-04-00	90-08-02	89-11-00
Jagst	74-06-20	78-00-22	80-00-20	80-00-20

Table 5. Percentages of under- and over-estimations of the top 5 discharge events using various gauge densities (columns) with respect to the top 5 values using reference discharge for the three considered catchments (rows) using HBV. Caption of Table 4 shows how to interpret the numbers here.

5.6 Effects of removing subscale variability of precipitation on SHETRAN discharge

Effects of using lumped precipitation on the resulting discharge, i.e., mean precipitation value at each time step for all cells, were also investigated. The aim was to see the effects of subscale variability on runoff. While considering 10 largest peaks per catchment for the entire time period, NS efficiencies of these dropped to 0.77, 0.78 and 0.90 for Enz, Kocher and Jagst respectively. Almost all peaks were reduced in their magnitudes to 84%, 85% and 93% with respect to the ones produced by the model on average with the distributed reference precipitation. Most of the underestimation of the peaks were during winter that are likely to be snowmelt events. These are location/elevation dependent and it makes sense that using a lumped value of precipitation results in incorrect melt behavior. Overall, the tendency was towards reduced discharge when using lumped precipitation. This tendency is likely to be much higher when a single cell is used to represent the catchment i.e., a fully lumped model.

5.7 Effects of measurement error in precipitation on runoff

290 To test how measurement error affects the model discharge, precipitation with a measurement error of 10% of each observed value having a standard Normal distribution was used and then interpolated as well. There, it was observed that magnitude of under- and over-estimation of the peaks becomes more variable as compared to the reference but the bias remained the same as that compared to using precipitation with no error. Table 6 shows the effects for precipitation. Comparing these to Table 3, it can be concluded that the trends are not significantly different for the two cases. Similar to interpolations with no errors, the

295 ones with the largest number of samples have more values closer to the reference precipitation. These results corroborate the conclusions by Balin et al. (2010); Lee et al. (2010).

These results have an interesting consequence. If the gauges have measurement errors that are Normally distributed i.e., cheaper gauges, such as the Netatmo personal weather stations, can be used to close the gap of missing precipitation due to sparse distribution networks. Studies, such as those by de Vos et al. (2017, 2019); Bárdossy et al. (2021), have shown that

300 these alternative sources of data can augment the existing networks, while still having some drawbacks nonetheless. The type of measurement error by these can be further studied to validate their usefulness for rainfall-runoff modeling.

	M025	M050	M100	M150
Enz	71-11-18	46-32-22	54-22-24	24-50-26
Kocher	80-09-11	66-18-16	46-34-20	38-34-28
Jagst	82-11-07	60-16-24	48-30-22	30-40-30

Table 6. Percentages of under- and over-estimations of the top 5 precipitation events using various gauge densities (columns) with respect to the top 5 values using reference precipitation for the three considered catchments (rows). The values are of the format *percentage of underestimations (below 97.5%), within a threshold of $\pm 2.5\%$, and overestimations (above 102.5%) with respect to the reference precipitation.* For example, 38-34-28 in the second row and last column means that out of the 10 interpolations (with 5 events per interpolation) using 150 points for Kocher, 38% of the events were below 97.5%, 34% were within 97.5% and 102.5%, and 28% were above 102.5% of the top 5 events using the reference precipitation.

6 Preliminary attempts to correct precipitation bias

Consistent bias was shown by the interpolated precipitation. Consequently, it was also tried to rectify it by transforming precipitation in such a manner where an improvement in the discharge could be observed. Two different approaches were

305 tested. These are described as follows.

Static transform of the form,

$$P'(t) = \begin{cases} P(t) & \text{if } P(t) < \psi, \\ \beta(P(t) - \psi)^{\gamma} & \text{else} \end{cases} \tag{1}$$

where, ψ is a threshold for transformation. β is a multiplier while γ is an exponent that may transform the values above the threshold linearly or non-linearly.

310   Using transforms that do not consider the time of the year or the type of weather during a precipitation event are also not optimal. For example, precipitation events in Summer are more intense, occur for a shorter period of time, are more abrupt in nature and cover smaller areas as compared to winter where the intensity is less, occur for longer periods of time, and cover much larger areas. Accounting for such information while correcting for bias can be useful. Hence, transformations based on weather circulation patterns (CPs) were used to correct the precipitation bias based on the type of event. An automatic CP

315   classification method based on Fuzzy logic (Bárdossy et al., 2002) was used to find relevant CPs that were dominant in the study area. The procedure assigns a type of weather to each time step based on the atmospheric pressure in and around the catchment area and some other constraints. The number of CPs that may be obtained is arbitrary. For this study 5 CPs were chosen based on previous experience and also for avoiding too many free variables for calibration. The transfomation was then applied to precipitation that took place only in the two CPs that were related to the wettest weather. Contrary to a static

320   transform based on the precipitation magnitude only, independent of time or weather, transforms are applied to each time step based on its CP, which depends on the weather and time of the year. The CP-based transform was as follows,

$$P'(t) = \beta_{CP} \cdot P(t)^{\gamma_{CP}} \tag{2}$$

where, β_{CP} is a CP dependent multiplier and γ_{CP} is a CP dependent exponent.

Finally, a simple experiment was set up to search for a consistent pattern in the unknown terms of the transforms using

325   the lumped HBV. The method to find the optimal transformation involved applying the same transform to precipitation values for all catchment while optimizing their model parameters independently. The assumption being that the model efficiencies will bring better performance compared to the case where no precipitation correction was considered. This lead to a problem of optimization in higher dimensions. For the previous cases, the optimization of model parameters was carried out for each catchment independently, which was an 11 dimensional problem. For the case of testing transforms, the model parameters

330   of the three catchments and the unknown transform parameters have to optimized simultaneously. This has to be the case, as optimizing transforms for each catchment will lead to them being very different than the neighbors. However, considering the behavior of precipitation in space, it could be argued that each catchment should be treated individually, but here the aim was to evaluate if an overall correction was possible. Hence, 36 parameters for the static-transform case and 37 for the CP-based case had to be optimized. For the case of the static transform, slight improvement in the results was observed for all the

335   catchments but no consistent patterns were observed, same was the case for the CP-based. Strangely, all transforms resulted in the reduction of the high precipitation values. Which signifies that the problem of the large precipitation's underestimation

cannot be considered independently of the low and medium precipitation values. Similar approaches and more sophisticated ones will be investigated in later research.

7   Summary and conclusions

340   An often ignored problem of peak flow underestimation in rainfall-runoff modeling by using interpolated data was investigated in this study. To do so, data were interpolated using different gauge densities. It was shown how interpolated precipitation differs from reference precipitation. This may come as no surprise as interpolation produces smooth transitions between two or more points that are very unlikely to represent the actual state of the variable in space-time. SHETRAN was used as a reference model that was assumed to represent reality with reconstructed precipitation as input. The other model was HBV. Runoff from
345   SHETRAN was chosen as a reference to avoid inherent mismatch of mass balances as compared to using observed discharge series. Simple approaches for bias correction were also presented, where it was learned that the bias cannot be corrected using simple static or weather dependent transforms of input precipitation.

We arrived at the following answers to the questions that were stated in the beginning:

1. Sampling density of stations in and around a catchment have profound effects on the quality of interpolated precipitation.
350   While it is obvious that more stations lead to better estimates of precipitation, it was recognized that low density leads to a more frequent high underestimation of areal precipitation, especially for the large events. Depending on the density the worst-case was an underestimation of about 75% of the precipitation volume. This effect decreased as the sampling density increased.

2. Both considered hydrological models showed a consequent underestimation of peak flows. For example, SHETRAN
355   produced a peak that was about 50% less compared to the case when reference precipitation was used. HBV did not show a similar loss comparatively as it was recalibrated each time for different precipitation but its performance deteriorated nonetheless.

3. Similar to previous studies, the effects of random measurement errors in precipitation on model discharge were not significant.

360   4. Using precipitation as input with no spatial variability, showed an overall loss in model performance, especially for the events that involved snowmelt.

Further conclusions that can be derived from the above mentioned results are:

1. While modeling in hydrology, variables should be modeled in space and time at the correct resolution to have usable results. Disregarding spatial characteristics (in terms of variance) leads to problems that cannot be solved by any model
365   or finer resolution temporal data.

2. Cheaper networks may prove valuable where observations are sparse if the condition that their measurement errors are normally distributed is met.

14

3. Finally, the results and conclusions of this study must be interpreted with the important fact in mind, that *models* were used to demonstrate the effects of the underestimation of peaks due to sparse networks and interpolations. In reality, it could very well be that these effects become less dominant/observable due any number of other reasons such as incorrect temperature or discharge readings; or using models that insufficiently represent all the processes the lead to river flows or changes in it. Nevertheless, this study proves that the main culprit behind underestimation of peaks is the observation network density provided that a model is used that has a description of the dominant rainfall-runoff producing mechanisms in it. The models used to demonstrate the effects are circumstantial to a large extent as the peak flow underestimation is due to the missing volume of input precipitation.

In future research, the following issues could be addressed:

1. Underestimation of intense precipitation due to interpolation.

2. Sensitivity of other variables, such as temperature, to interpolation and their effects on runoff. Especially, catchments with seasonal or permanent snow cover.

3. The magnitude of performance compensation that recalibration introduces due to the missing precipitation.

4. The effects of using different density networks on calibrated model parameters and regionalization of model parameters.

5. Determining the error distributions of cheaper precipitation gauges to establish their usefulness in rainfall-runoff modeling.

References

395 Shakeel Ahmed and Ghislain De Marsily. Comparison of geostatistical methods for estimating transmissivity using data on transmissivity and specific capacity. *Water Resources Research*, 23(9):1717–1737, 1987. https://doi.org/https://doi.org/10.1029/WR023i009p01717.

Daniela Balin, Hyosang Lee, and Michael Rode. Is point uncertain rainfall likely to have a great impact on distributed complex hydrological modeling? *Water Resources Research*, 46(11), 2010. https://doi.org/https://doi.org/10.1029/2009WR007848. URL https://agupubs.onlinelibrary.wiley.com/doi/abs/10.1029/2009WR007848.

400 A. Bárdossy and T. Das. Influence of rainfall observation network on model calibration and application. *Hydrology and Earth System Sciences*, 12(1):77–89, 2008. https://doi.org/10.5194/hess-12-77-2008. URL https://hess.copernicus.org/articles/12/77/2008/.

A. Bárdossy, J. Seidel, and A. El Hachem. The use of personal weather station observations to improve precipitation estimation and interpolation. *Hydrology and Earth System Sciences*, 25(2):583–601, 2021. https://doi.org/10.5194/hess-25-583-2021. URL https://hess.copernicus.org/articles/25/583/2021/.

405 András Bárdossy, Jiri Stehlík, and Hans-Joachim Caspary. Automated objective classification of daily circulation patterns for precipitation and temperature downscaling based on optimized fuzzy rules. *Climate Research*, 23(1):11–22, 2002. https://doi.org/10.3354/cr023011.

S. Bergström. *The HBV Model: Its Structure and Applications*. SMHI Reports Hydrology. SMHI, 1992. URL https://books.google.de/books?id=u7F7mwEACAAJ.

Keith Beven. An epistemically uncertain walk through the rather fuzzy subject of observation and model uncertainties1. *Hydrological*
410 *Processes*, 35(1):e14012, 2021. https://doi.org/https://doi.org/10.1002/hyp.14012. URL https://onlinelibrary.wiley.com/doi/abs/10.1002/hyp.14012.

Stephen J Birkinshaw, Philip James, and John Ewen. Graphical user interface for rapid set-up of shetran physically-based river catchment model. *Environmental Modelling & Software*, 25(4):609–610, 2010.

András Bárdossy and Geoffrey Pegram. Interpolation of precipitation under topographic influence at different time scales. *Water Resources*
415 *Research*, 49(8):4545–4565, 2013. https://doi.org/https://doi.org/10.1002/wrcr.20307. URL https://agupubs.onlinelibrary.wiley.com/doi/abs/10.1002/wrcr.20307.

András Bárdossy, Faizan Anwar, and Jochen Seidel. Hydrological modelling in data sparse environment: Inverse modelling of a historical flood event. *Water*, 12(11), 2020. ISSN 2073-4441. https://doi.org/10.3390/w12113242. URL https://www.mdpi.com/2073-4441/12/11/3242.

420 András Bárdossy, Ehsan Modiri, Faizan Anwar, and Geoffrey Pegram. Gridded daily precipitation data for iran: A comparison of different methods. *Journal of Hydrology: Regional Studies*, 38:100958, 2021. ISSN 2214-5818. https://doi.org/https://doi.org/10.1016/j.ejrh.2021.100958. URL https://www.sciencedirect.com/science/article/pii/S2214581821001877.

András Bárdossy, Chris Kilsby, Stephen Birkinshaw, Ning Wang, and Faizan Anwar. Is precipitation responsible for the most hydrological model uncertainty? *Frontiers in Water*, 4, 2022. ISSN 2624-9375. https://doi.org/10.3389/frwa.2022.836554. URL
425 https://www.frontiersin.org/article/10.3389/frwa.2022.836554.

L. de Vos, H. Leijnse, A. Overeem, and R. Uijlenhoet. The potential of urban rainfall monitoring with crowdsourced automatic weather stations in amsterdam. *Hydrology and Earth System Sciences*, 21(2):765–777, 2017. https://doi.org/10.5194/hess-21-765-2017. URL https://hess.copernicus.org/articles/21/765/2017/.

Lotte Wilhelmina de Vos, Hidde Leijnse, Aart Overeem, and Remko Uijlenhoet. Quality control for crowdsourced personal weather stations to enable operational rainfall monitoring. *Geophysical Research Letters*, 46(15):8820–8829, 2019. https://doi.org/https://doi.org/10.1029/2019GL083731. URL https://agupubs.onlinelibrary.wiley.com/doi/abs/10.1029/2019GL083731.

DWD. https://opendata.dwd.de/climate_environment/CDC/observations_germany/climate/daily/, 2019 2019.

John Ewen, Geoff Parkin, and Patrick Enda O'Connell. Shetran: distributed river basin flow and transport modeling system. *Journal of hydrologic engineering*, 5(3):250–258, 2000.

Tom G. Farr, Paul A. Rosen, Edward Caro, Robert Crippen, Riley Duren, Scott Hensley, Michael Kobrick, Mimi Paller, Ernesto Rodriguez, Ladislav Roth, David Seal, Scott Shaffer, Joanne Shimada, Jeffrey Umland, Marian Werner, Michael Oskin, Douglas Burbank, and Douglas Alsdorf. The shuttle radar topography mission. *Reviews of Geophysics*, 45(2), 2007. https://doi.org/https://doi.org/10.1029/2005RG000183. URL https://agupubs.onlinelibrary.wiley.com/doi/abs/10.1029/2005RG000183.

G.H. Hargreaves and Z.A. Samani. Estimating potential evapotranspiration. *Journal of the Irrigation and Drainage Division*, 108(3): 225–230, 1982.

Charles R. Harris, K. Jarrod Millman, Stéfan J. van der Walt, Ralf Gommers, Pauli Virtanen, David Cournapeau, Eric Wieser, Julian Taylor, Sebastian Berg, Nathaniel J. Smith, Robert Kern, Matti Picus, Stephan Hoyer, Marten H. van Kerkwijk, Matthew Brett, Allan Haldane, Jaime Fernández del Río, Mark Wiebe, Pearu Peterson, Pierre Gérard-Marchant, Kevin Sheppard, Tyler Reddy, Warren Weckesser, Hameer Abbasi, Christoph Gohlke, and Travis E. Oliphant. Array programming with NumPy. *Nature*, 585(7825):357–362, September 2020. https://doi.org/10.1038/s41586-020-2649-2. URL https://doi.org/10.1038/s41586-020-2649-2.

J. D. Hunter. Matplotlib: A 2d graphics environment. *Computing in Science & Engineering*, 9(3):90–95, 2007. https://doi.org/10.1109/MCSE.2007.55.

Dmitri Kavetski, Stewart W. Franks, and George Kuczera. *Confronting Input Uncertainty in Environmental Modelling*, pages 49–68. American Geophysical Union (AGU), 2003. ISBN 9781118665671. https://doi.org/https://doi.org/10.1029/WS006p0049. URL https://agupubs.onlinelibrary.wiley.com/doi/abs/10.1029/WS006p0049.

Hyosang Lee, Daniela Balin, Rajesh Raj Shrestha, and Michael Rode. Streamflow prediction with uncertainty analysis, weida catchment, germany. *KSCE Journal of Civil Engineering*, 14(3):413–420, 2010.

David R. Legates and Cort J. Willmott. Mean seasonal and spatial variability in gauge-corrected, global precipitation. *International Journal of Climatology*, 10(2):111–127, 1990. https://doi.org/https://doi.org/10.1002/joc.3370100202. URL https://rmets.onlinelibrary.wiley.com/doi/abs/10.1002/joc.3370100202.

Elizabeth Lewis, Stephen Birkinshaw, Chris Kilsby, and Hayley J. Fowler. Development of a system for automated setup of a physically-based, spatially-distributed hydrological model for catchments in great britain. *Environmental Modelling & Software*, 108:102–110, 2018. ISSN 1364-8152. https://doi.org/https://doi.org/10.1016/j .envsoft.2018.07.006. URL https://www.sciencedirect.com/science/article/pii/S1364815216311331.

LUBW. https://udo.lubw.baden-wuerttemberg.de/public/, 2020.

Michael M McKerns, Leif Strand, Tim Sullivan, Alta Fang, and Michael AG Aivazis. Building a framework for predictive science. *arXiv preprint arXiv:1202.1056*, 2012.

Edom Moges, Yonas Demissie, Laurel Larsen, and Fuad Yassin. Review: Sources of hydrological model uncertainties and advances in their analysis. *Water*, 13(1), 2021. ISSN 2073-4441. https://doi.org/10.3390/w13010028. URL https://www.mdpi.com/2073-4441/13/1/28.

J.E. Nash and J.V. Sutcliffe. River flow forecasting through conceptual models. 1. a discussion of principles. *Journal of Hydrology*, 10: 282–290, 1970.

Earl L. Neff. How much rain does a rain gage gage? *Journal of Hydrology*, 35(3):213–220, 1977. ISSN 0022-1694. https://doi.org/https://doi.org/10.1016/0022-1694(77)90001-4. URL https://www.sciencedirect.com/science/article/pii/0022169477900014.

470 Benjamin Renard, Dmitri Kavetski, George Kuczera, Mark Thyer, and Stewart W. Franks. Understanding predictive uncertainty in hydrologic modeling: The challenge of identifying input and structural errors. *Water Resources Research*, 46(5), 2010. https://doi.org/https://doi.org/10.1029/2009WR008328. URL https://agupubs.onlinelibrary.wiley.com/doi/abs/10.1029/2009WR008328.

Rainer Storn and Kenneth Price. Differential evolution – a simple and efficient heuristic for global optimization over continuous spaces. *Journal of Global Optimization*, 11(4):341–359, 1997.

475 The pandas development team. pandas-dev/pandas: Pandas, feb 2020. URL https://doi.org/10.5281/zenodo.3509134.

G. van Rossum. Python tutorial. Technical Report CS-R9526, Centrum voor Wiskunde en Informatica (CWI), Amsterdam, May 1995.

Pauli Virtanen, Ralf Gommers, Travis E. Oliphant, Matt Haberland, Tyler Reddy, David Cournapeau, Evgeni Burovski, Pearu Peterson, Warren Weckesser, Jonathan Bright, Stéfan J. van der Walt, Matthew Brett, Joshua Wilson, K. Jarrod Millman, Nikolay Mayorov, Andrew R. J. Nelson, Eric Jones, Robert Kern, Eric Larson, C J Carey, İlhan Polat, Yu Feng, Eric W. Moore, Jake VanderPlas, Denis Laxalde, Josef

480 Perktold, Robert Cimrman, Ian Henriksen, E. A. Quintero, Charles R. Harris, Anne M. Archibald, Antônio H. Ribeiro, Fabian Pedregosa, Paul van Mulbregt, and SciPy 1.0 Contributors. SciPy 1.0: Fundamental Algorithms for Scientific Computing in Python. *Nature Methods*, 17:261–272, 2020. https://doi.org/10.1038/s41592-019-0686-2.

Wes McKinney. Data Structures for Statistical Computing in Python. In Stéfan van der Walt and Jarrod Millman, editors, *Proceedings of the 9th Python in Science Conference*, pages 56 – 61, 2010. https://doi.org/10.25080/Majora-92bf1922-00a.

485 Daqing Yang, Esko Elomaa, Asko Tuominen, Ari Aaltonen, Barry Goodison, Thilo Gunther, Valentin Golubev, Boris Sevruk, Henning Madsen, and Janja Milkovic. Wind-induced Precipitation Undercatch of the Hellmann Gauges. *Hydrology Research*, 30(1):57–80, 02 1999. ISSN 0029-1277. https://doi.org/10.2166/nh.1999.0004. URL https://doi.org/10.2166/nh.1999.0004.

Soni Yatheendradas, Thorsten Wagener, Hoshin Gupta, Carl Unkrich, David Goodrich, Mike Schaffner, and Anne Stewart. Understanding uncertainty in distributed flash flood forecasting for semiarid regions. *Water Resources Research*, 44(5), 2008.

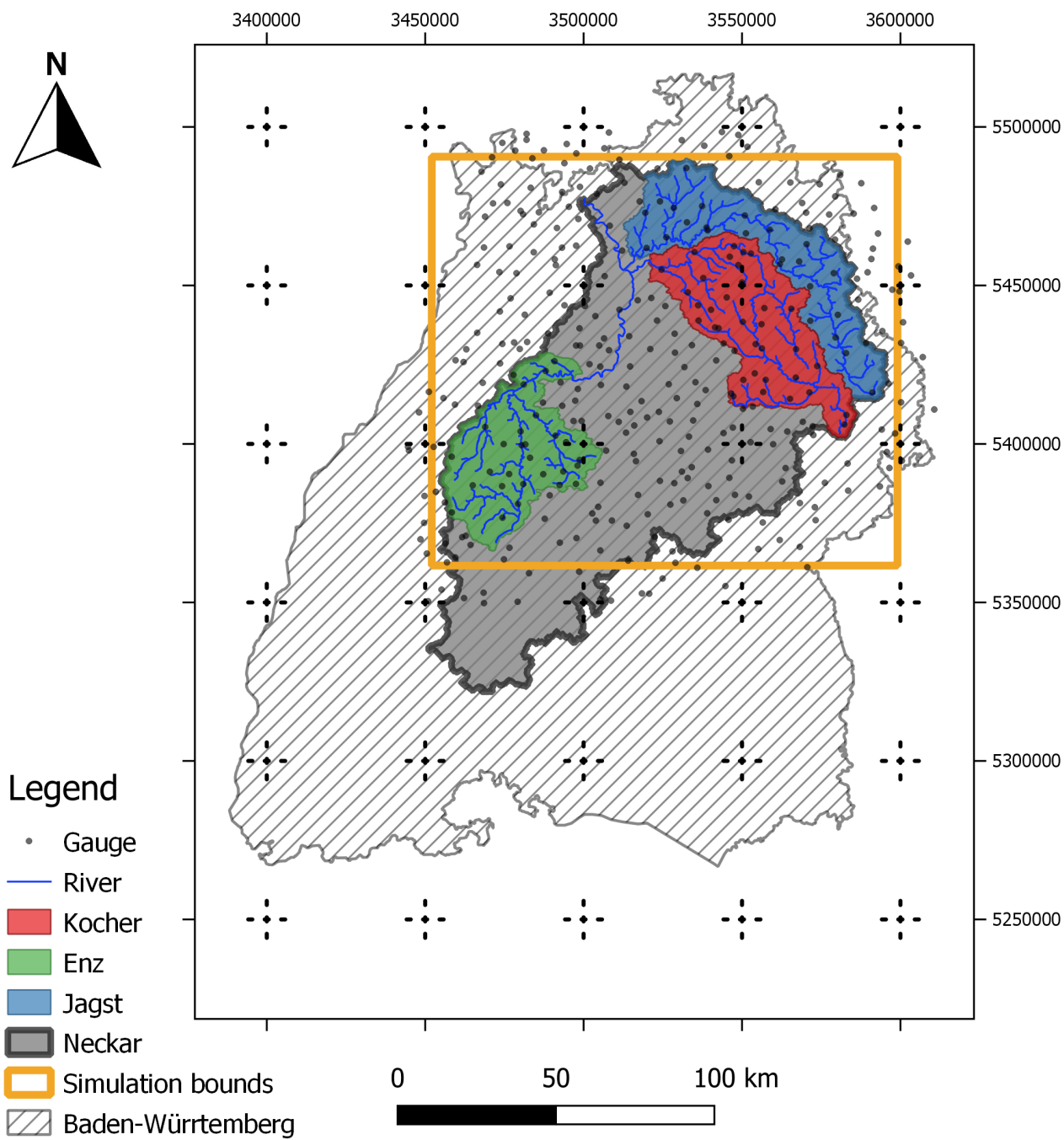490 https://doi.org/https://doi.org/10.1029/2007 WR005940. URL https://agupubs.onlinelibrary.wiley.com/doi/abs/10.1029/2007WR005940.
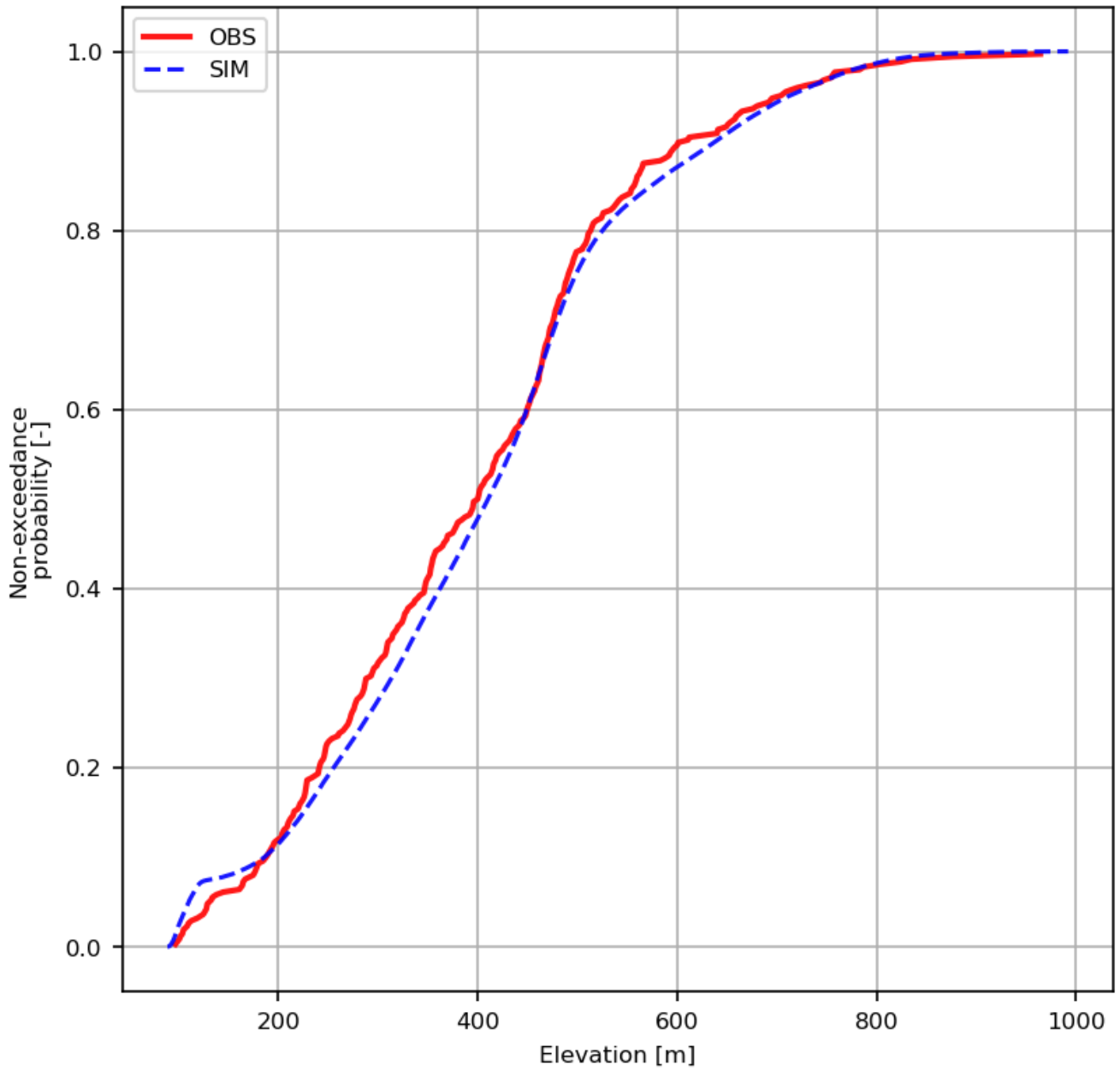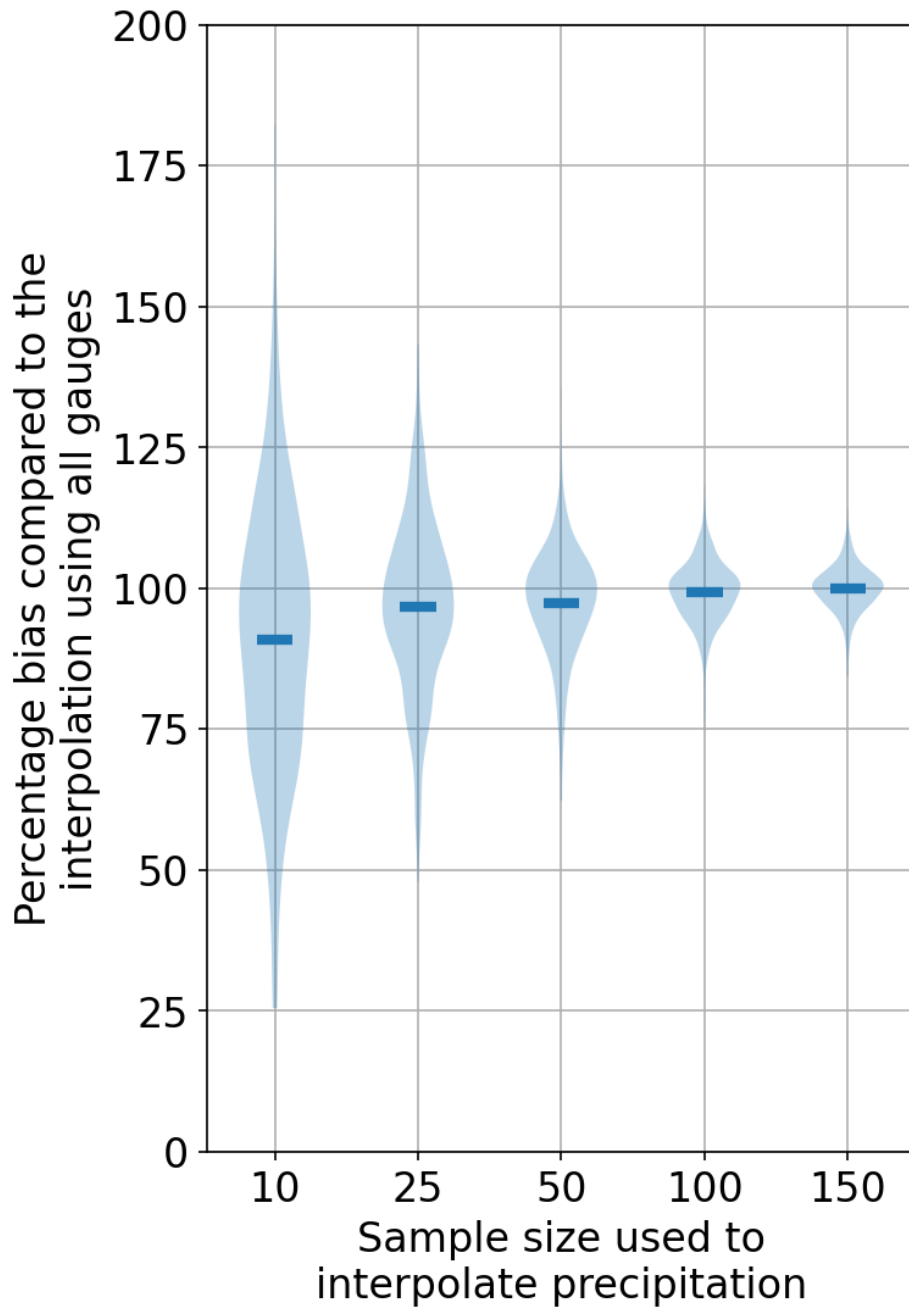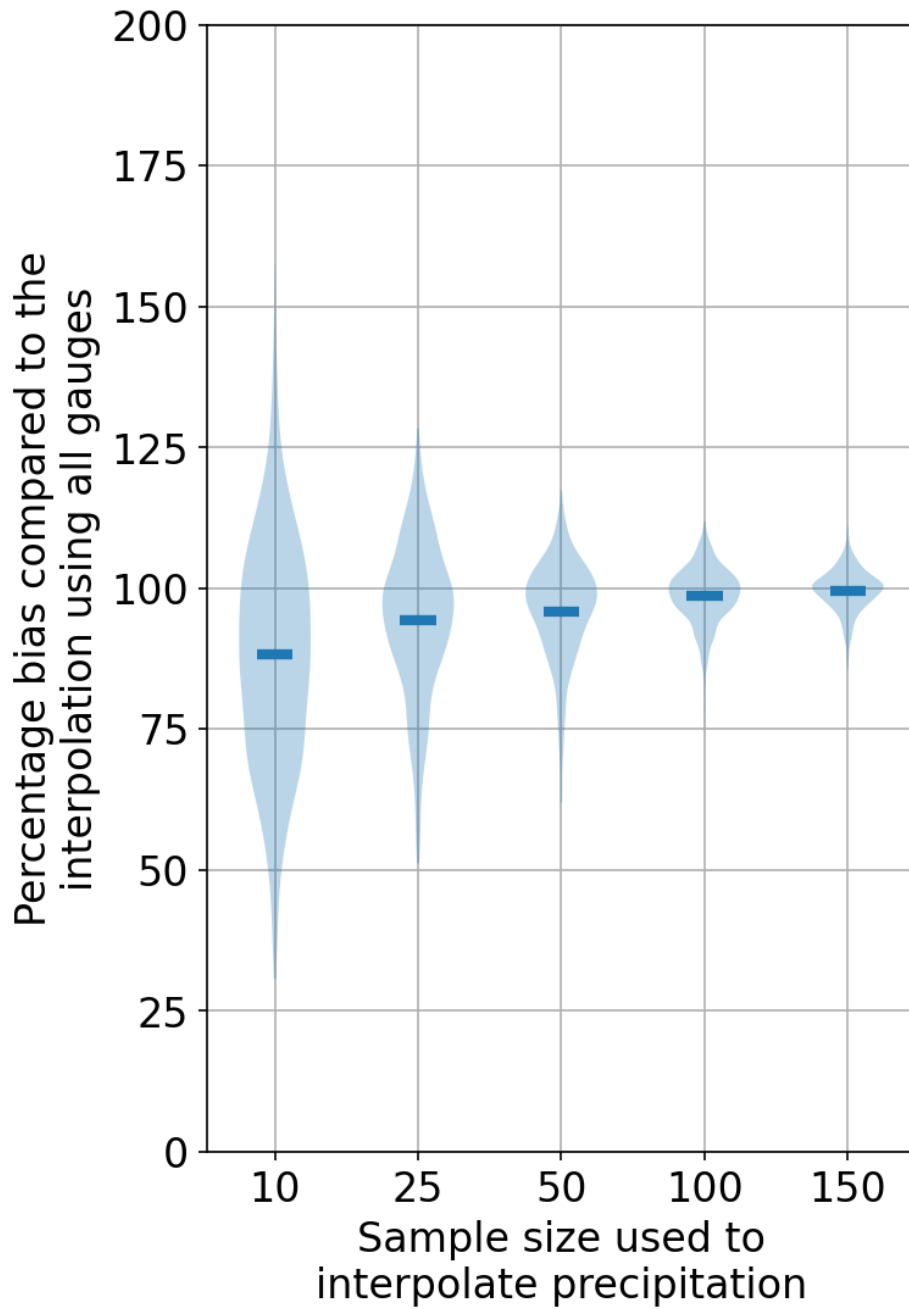
**Figure 1.** Study area (taken from Bárdossy et al. (2022))

Figure 2. Comparison of elevation distributions of observation locations (red) and the whole simulation grid (blue) using the SRTM 90m grid for the study area.
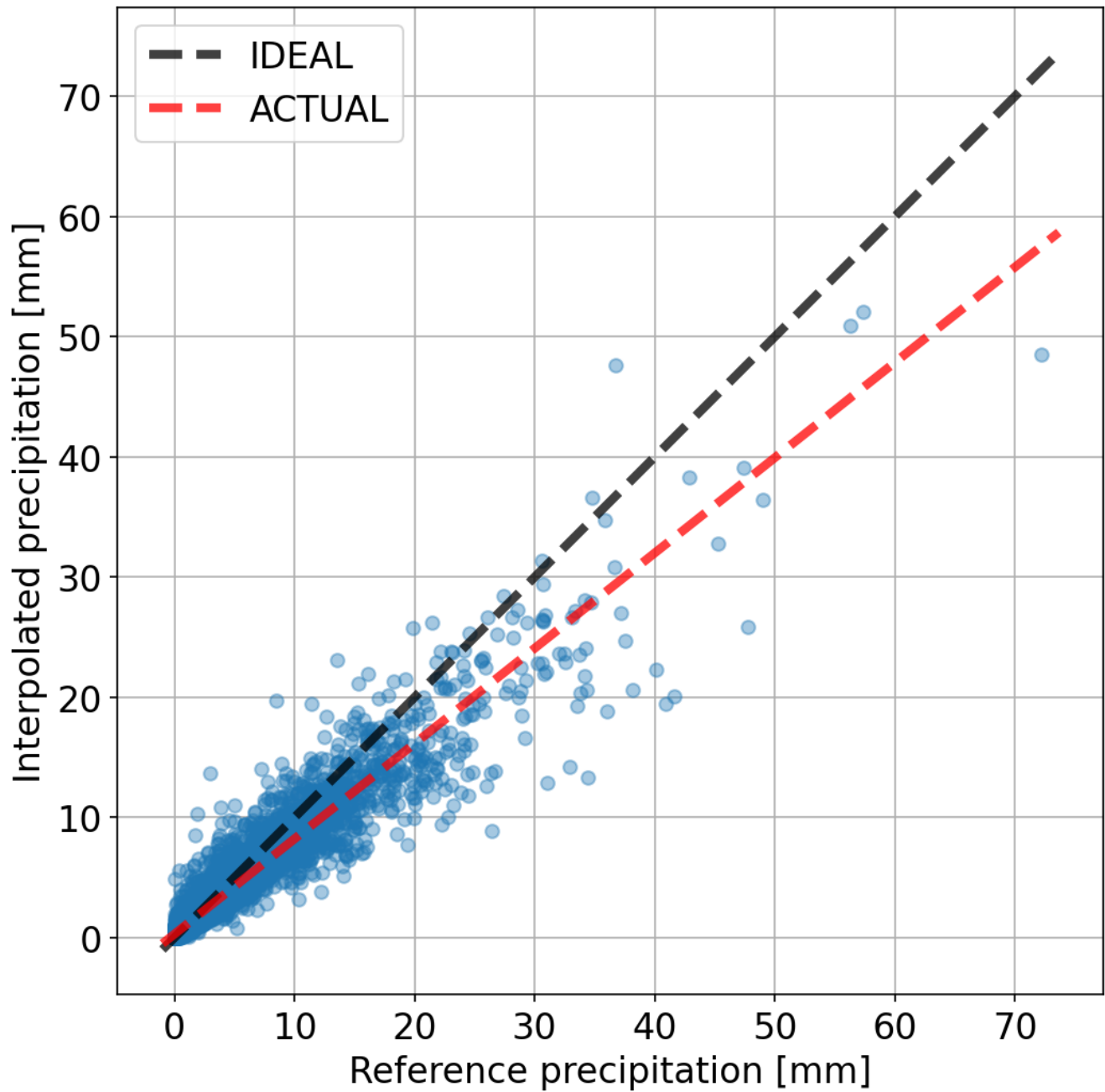
Figure 3. Precipitation bias comparison of the top five largest values due to using fewer points against an interpolation that uses all the points using NN.
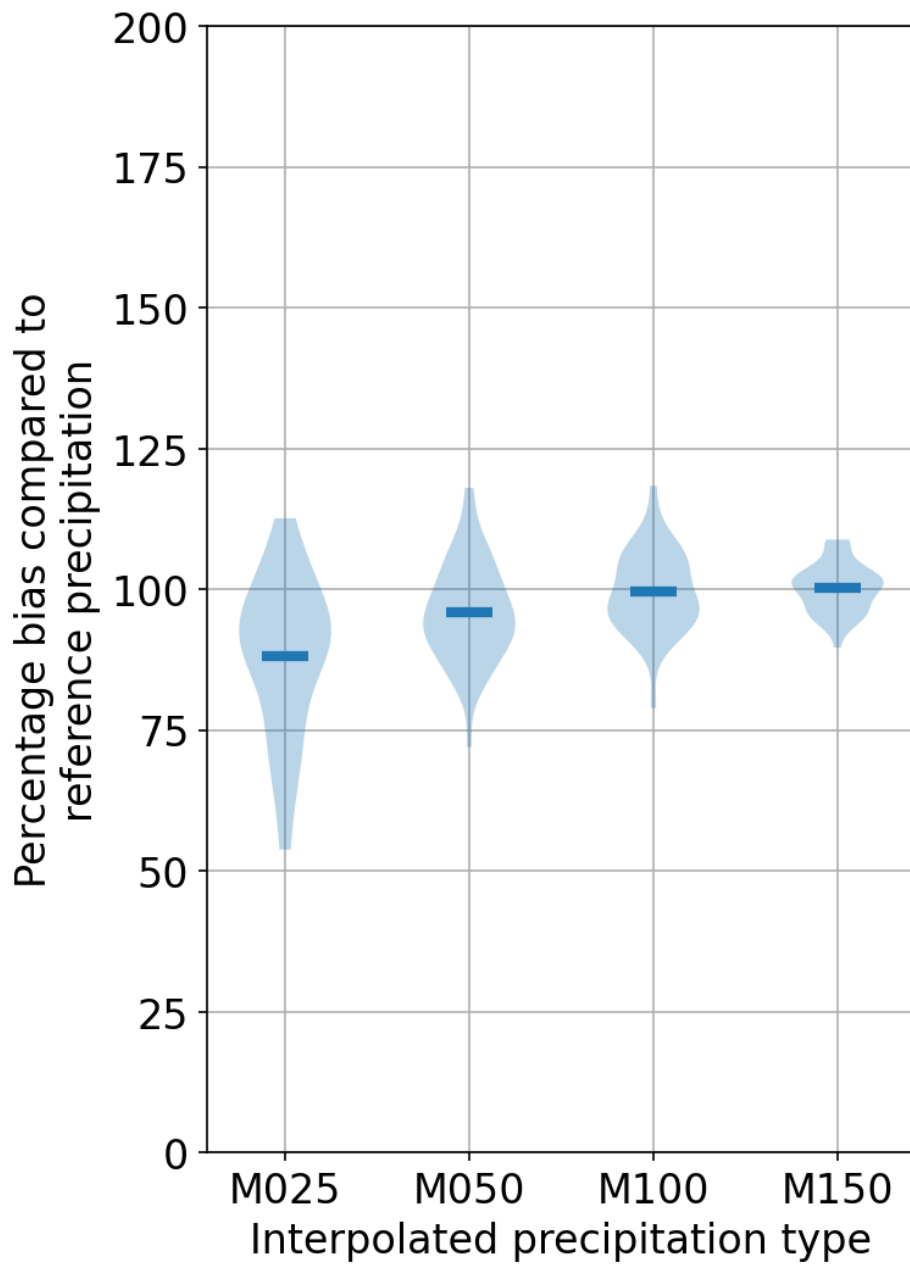
Figure 4. Precipitation bias comparison of the top five largest values due to using fewer points against an interpolation that uses all the points using OK.
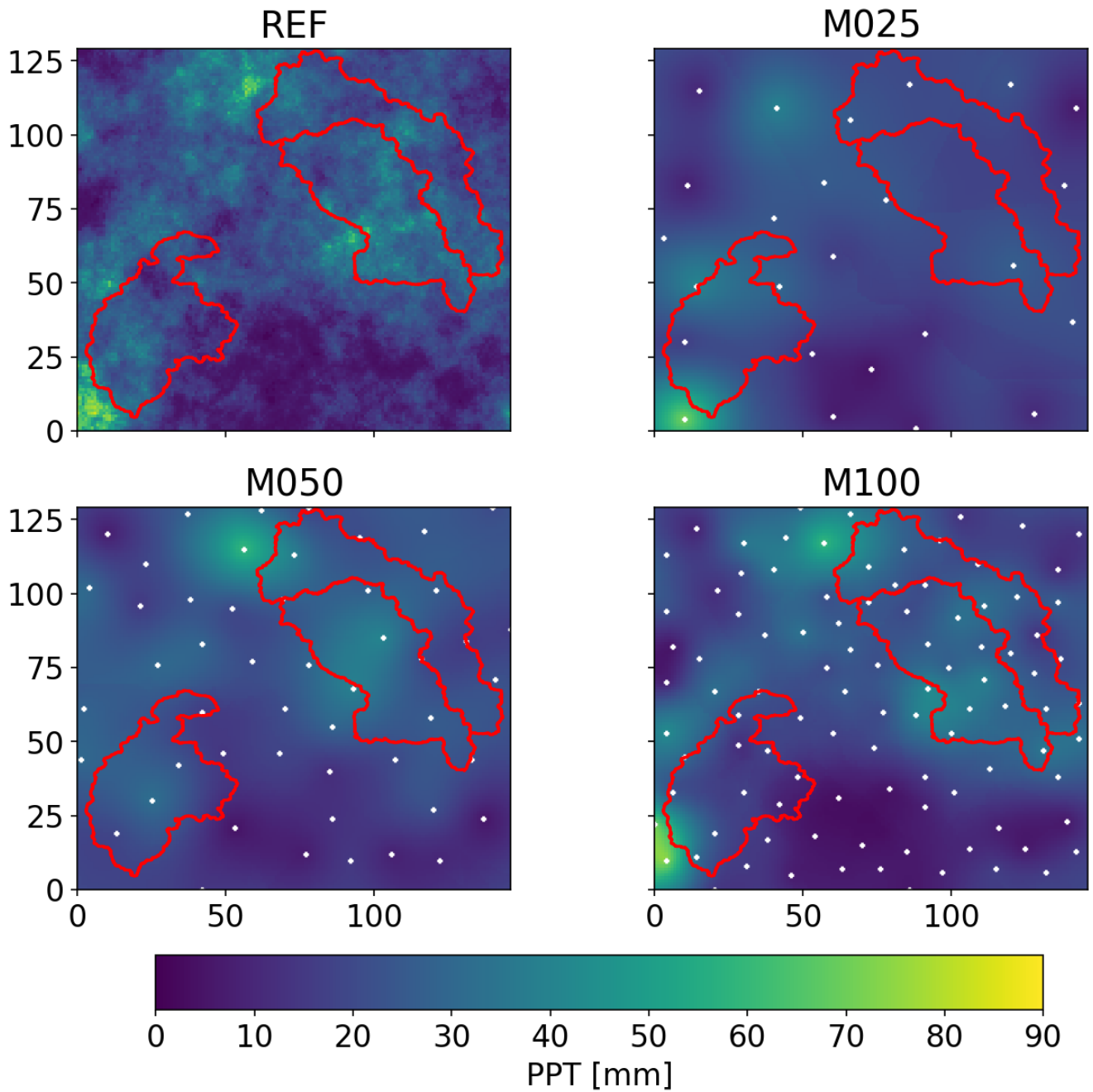
Figure 5. Comparison of precipitation interpolations for a time step with high precipitation with the reference.

Figure 6. Scatter of reference and lumped interpolated precipitation for one catchment.

Figure 7. Precipitation bias comparison of various interpolations with respect to the reference for the top five largest values.
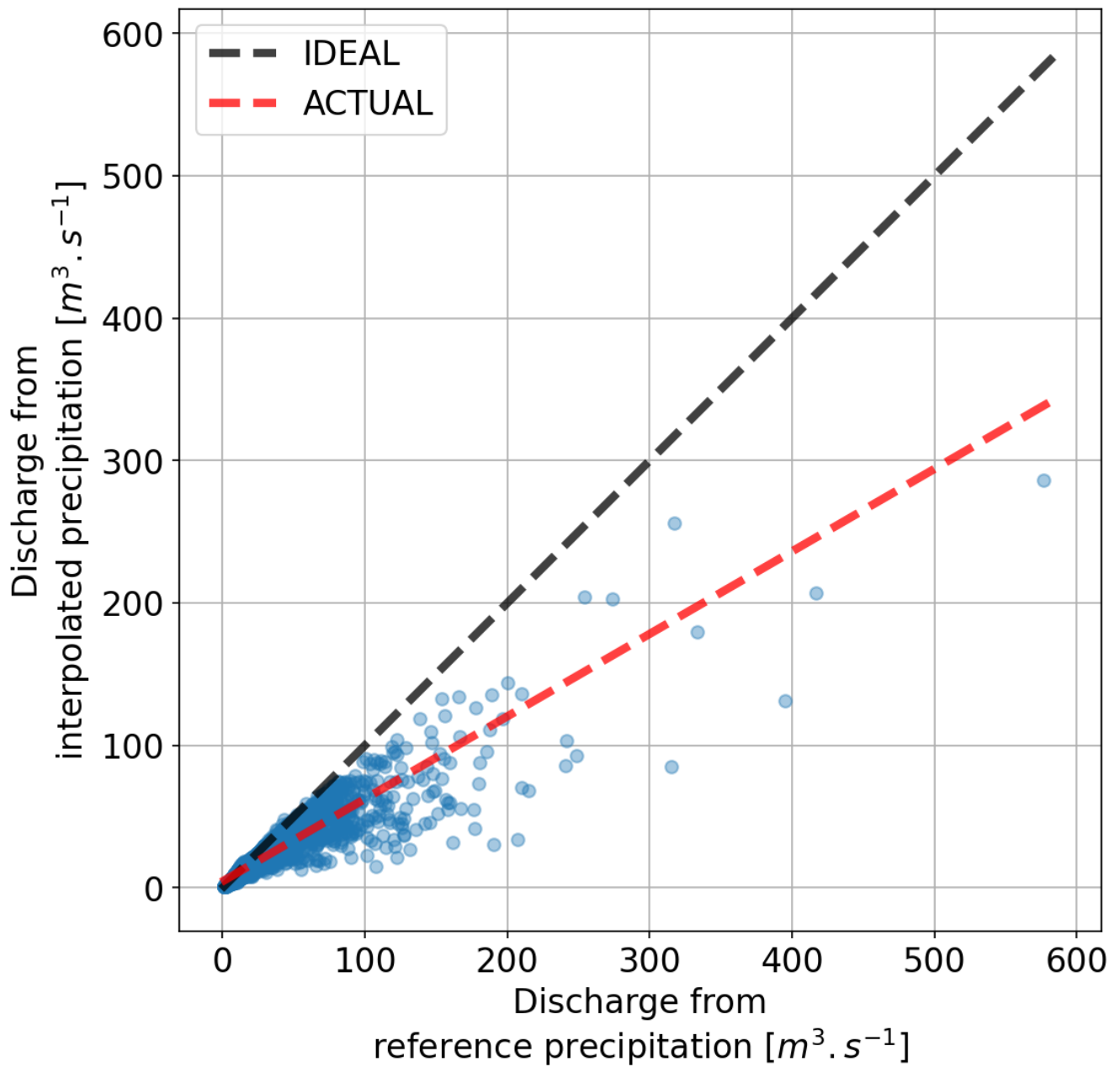
Figure 8. Scatter of discharge using reference and interpolated precipitation for one catchment using SHETRAN.
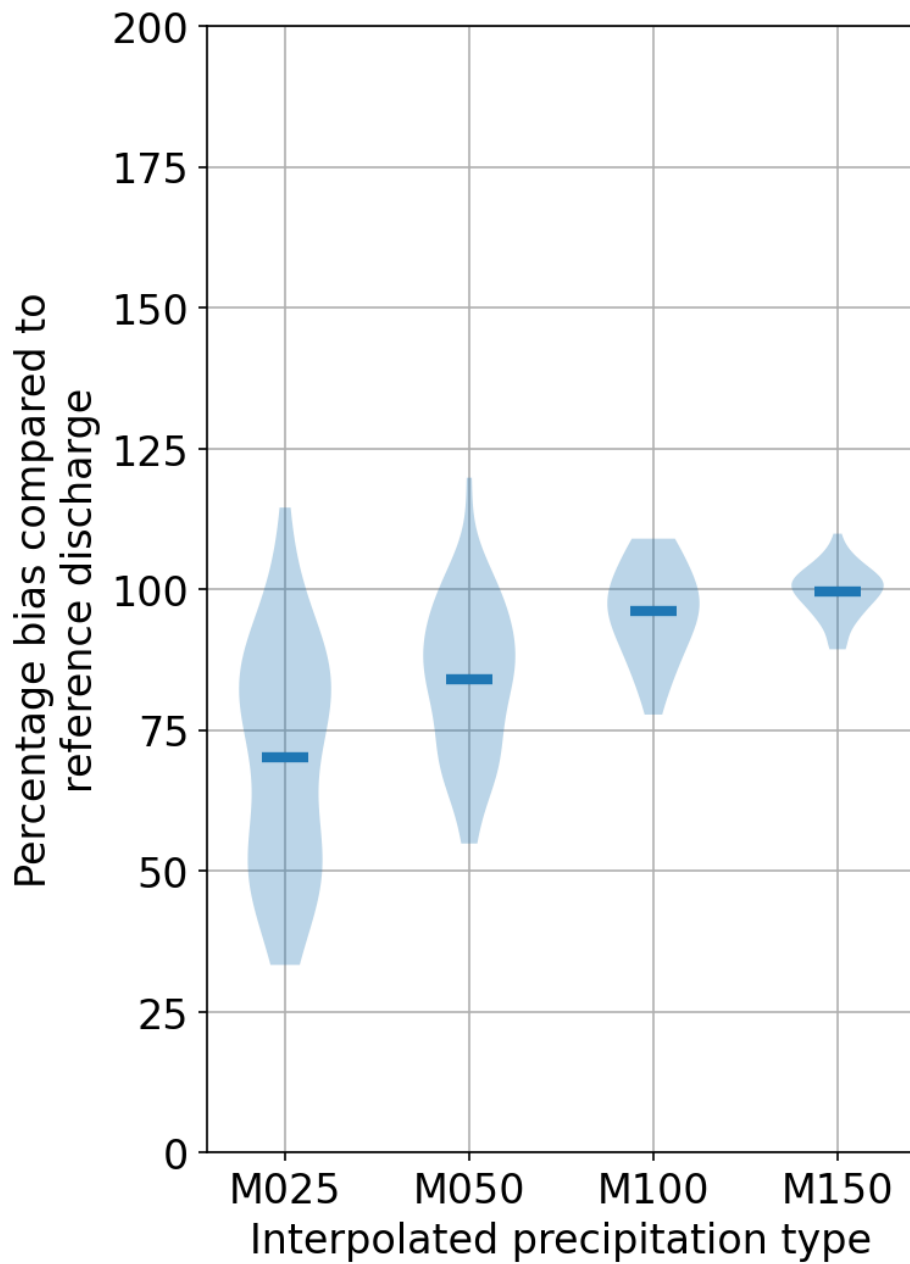
Figure 9. Discharge bias comparison of various interpolations with respect to the reference for the top five largest values using SHETRAN.
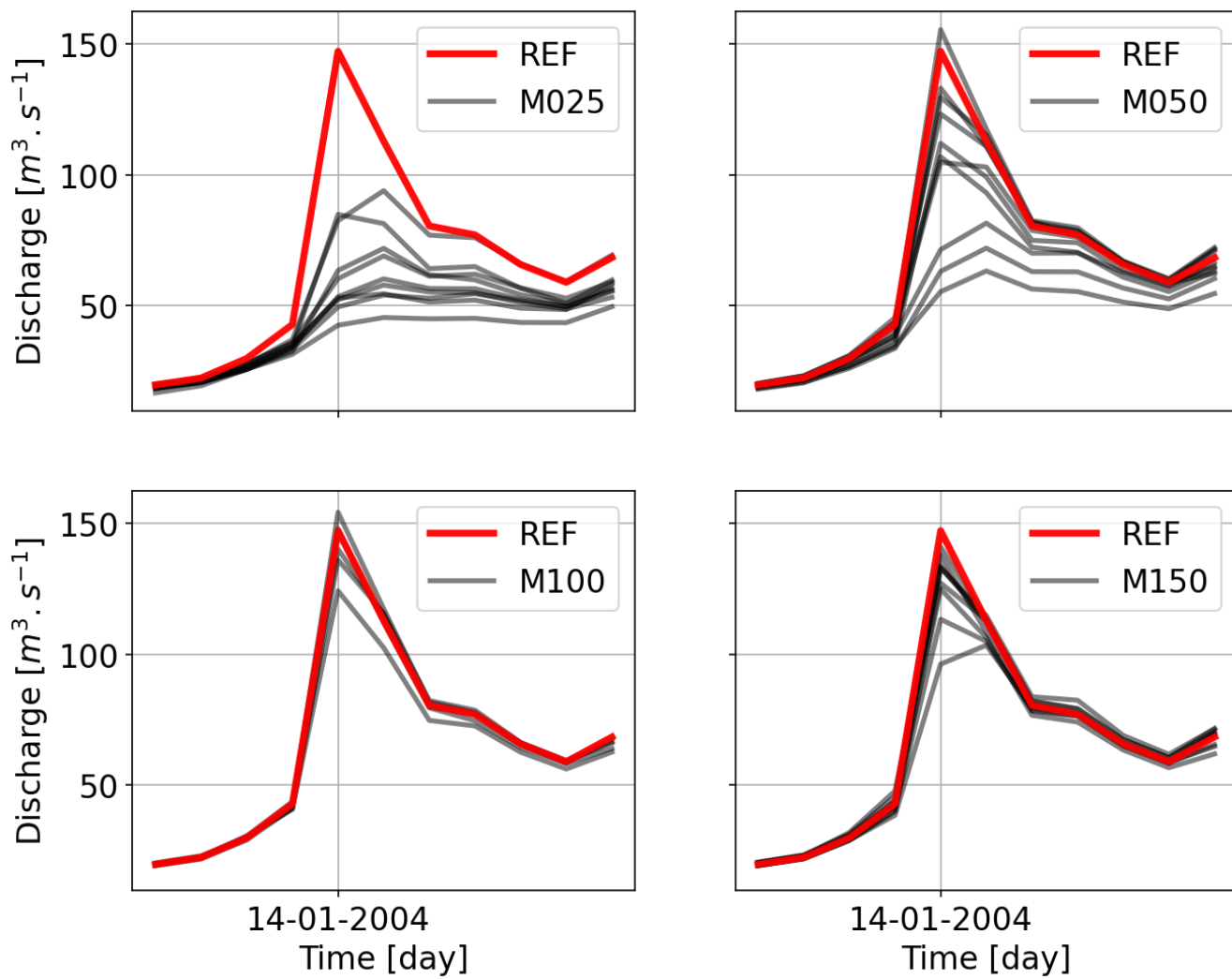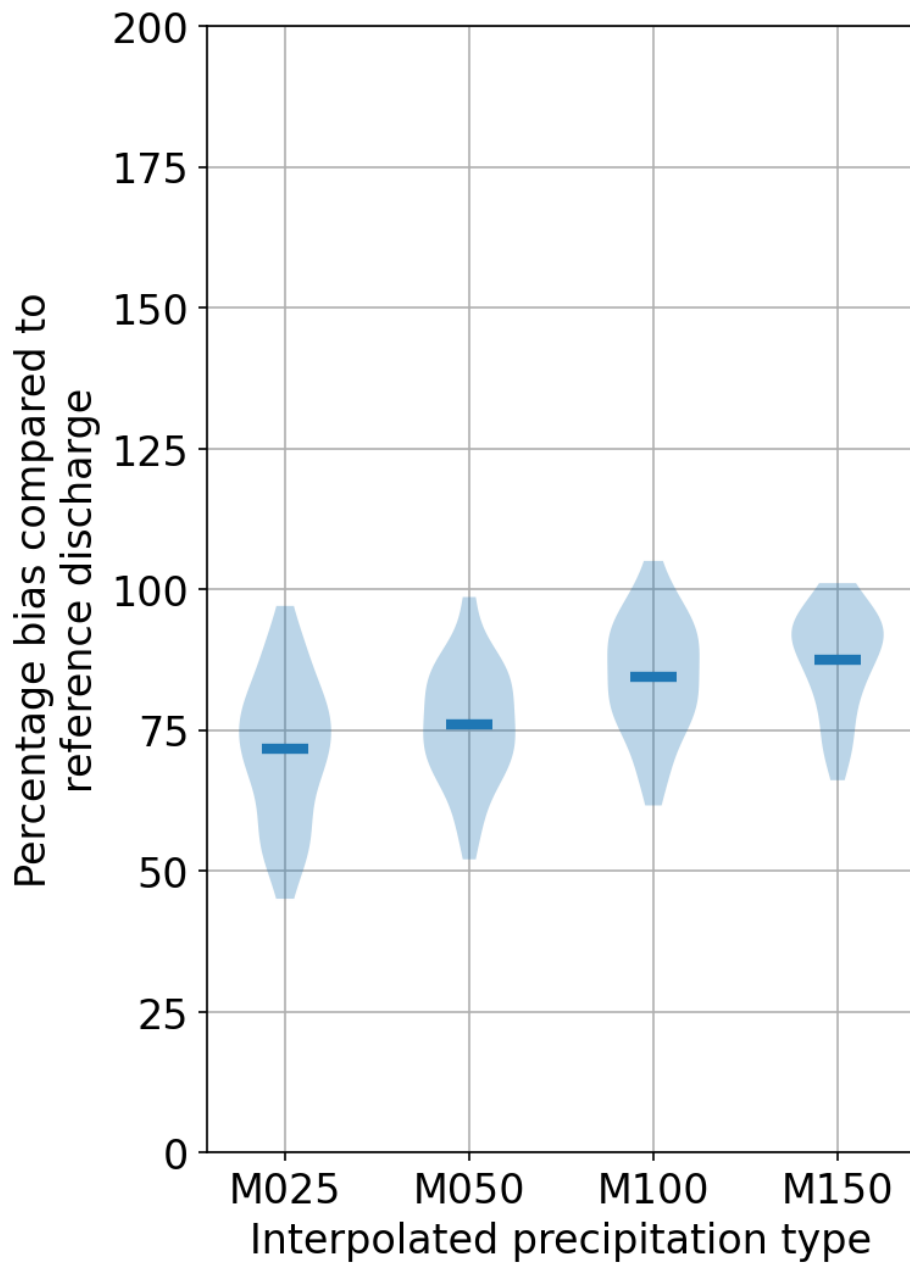
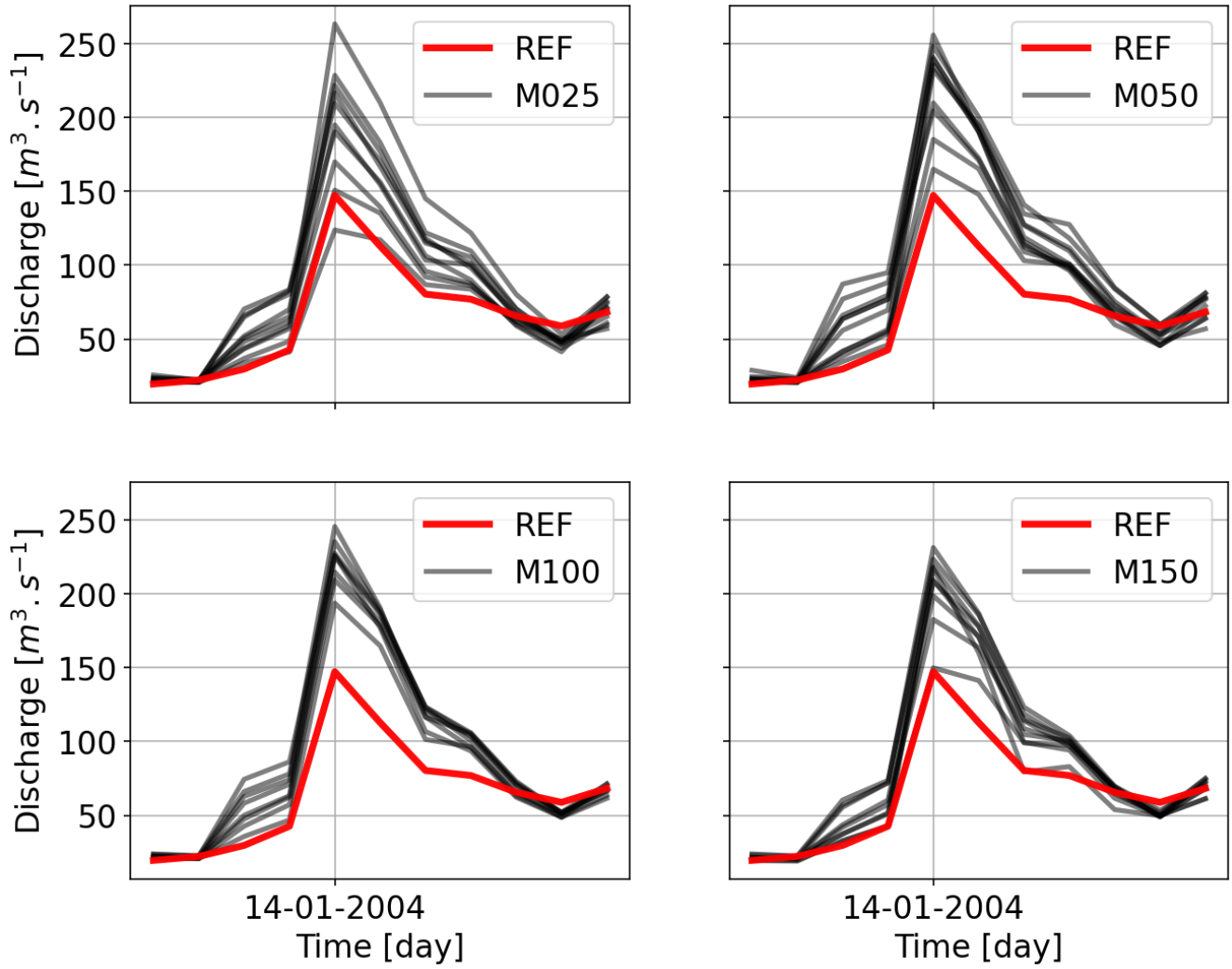**Figure 10.** Event hydrograph comparison for various gauging densities using SHETRAN.
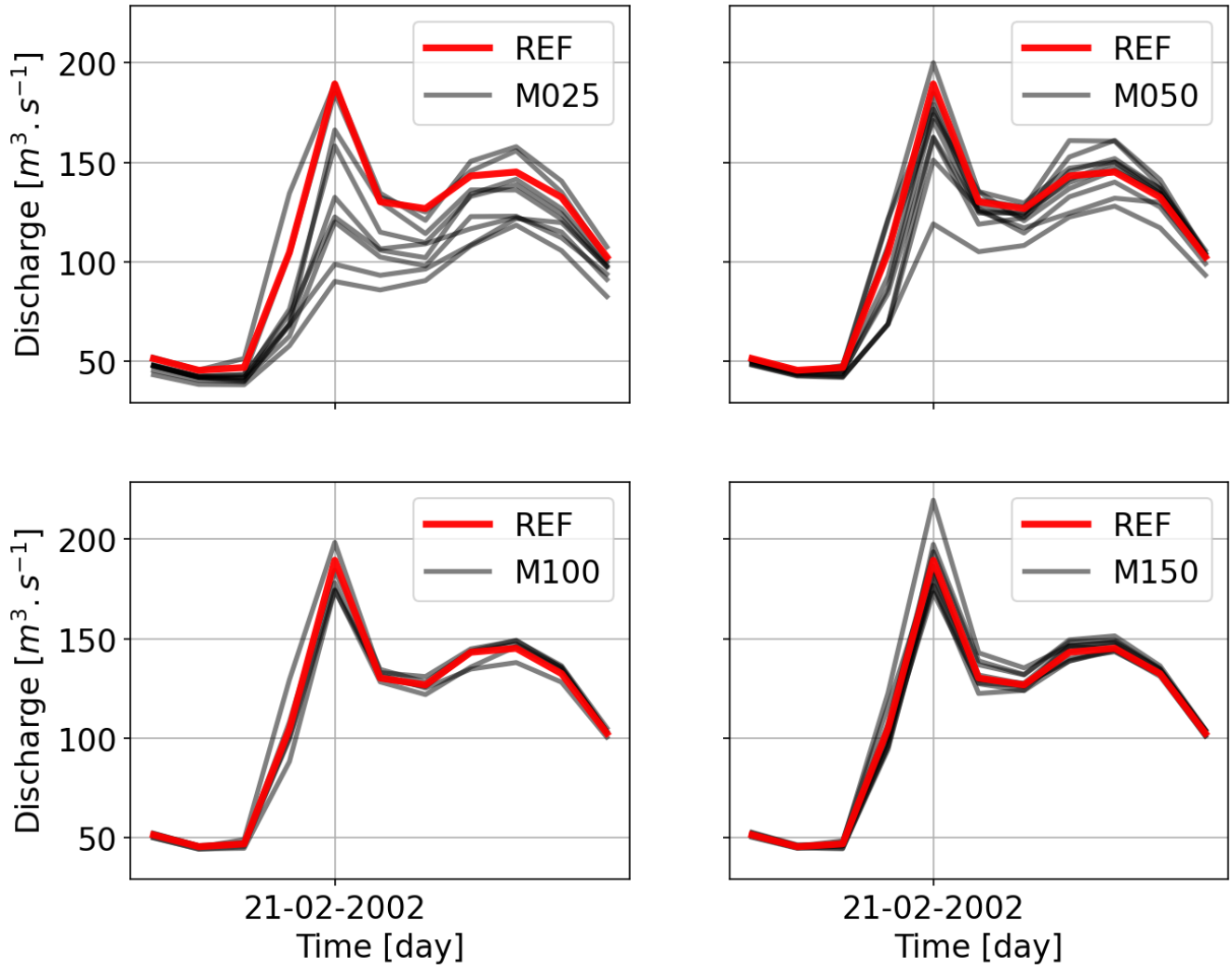
Figure 11. Event hydrograph comparison for various gauging densities using SHETRAN.
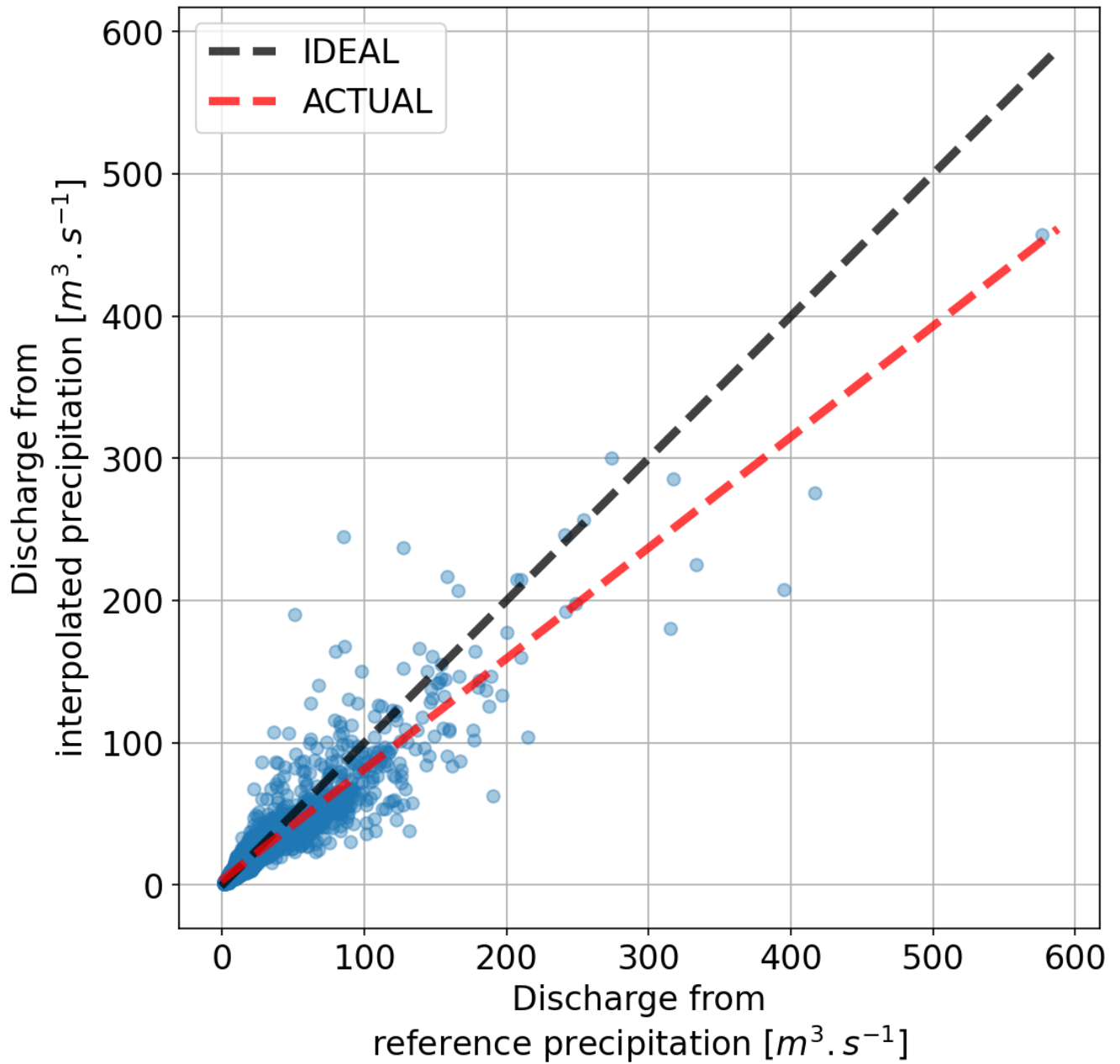
Figure 12. Scatter of discharge using reference and interpolated precipitation for one catchment using HBV.
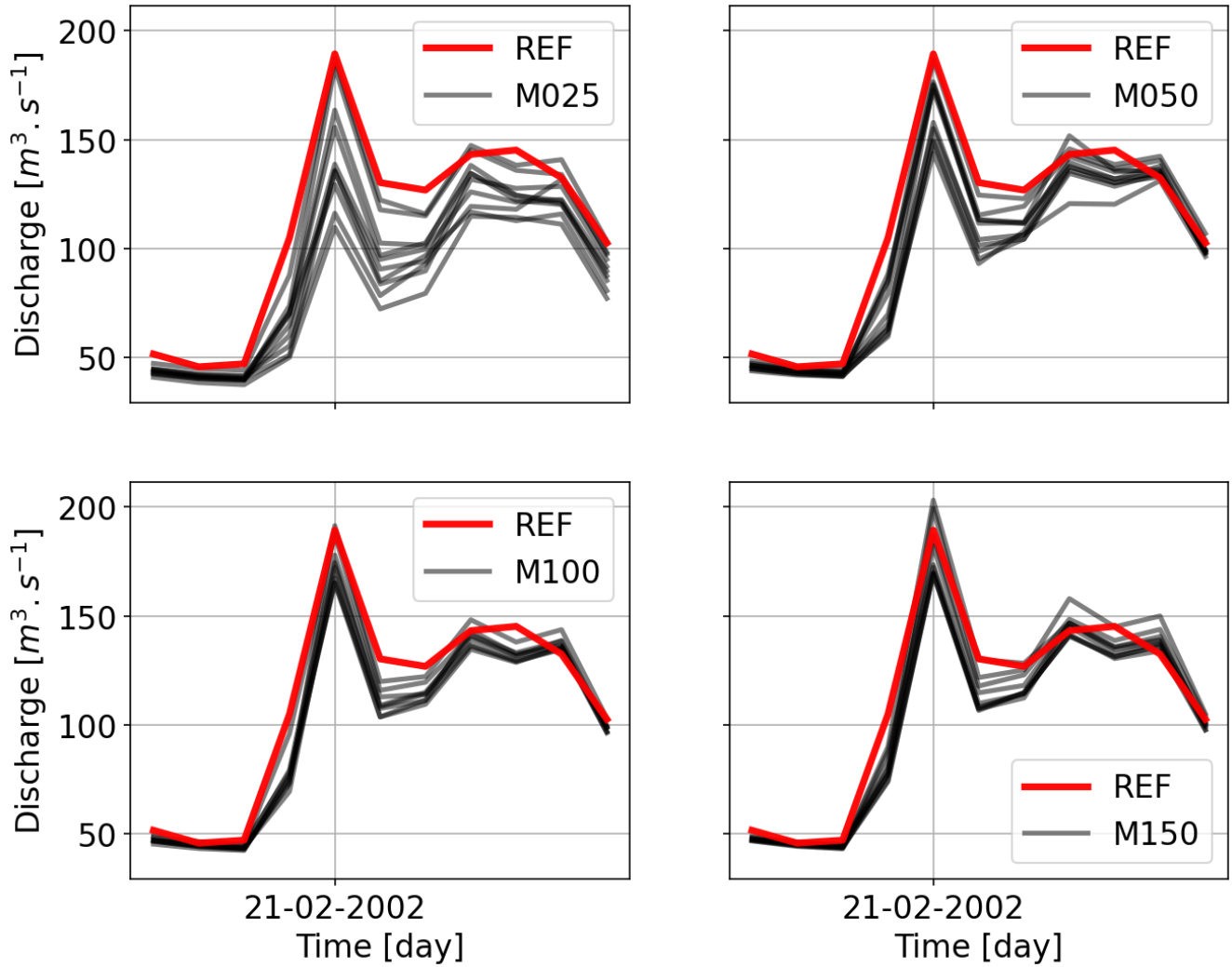
Figure 13. Discharge bias comparison of various interpolations with respect to the reference for the top five largest values using HBV.

Figure 14. Event hydrograph comparison for various gauging densities using HBV.

Figure 15. Event hydrograph comparison for various gauging densities using HBV.